Journal of Electrical Engineering & Technology (2024) 19:2817–2829
https://doi.org/10.1007/s42835-024-01864-1

ORIGINAL ARTICLE

A Study on LSTM-Based Lithium Battery SoH Estimation in Urban Railway Vehicle Operating Environments

Hyo Seok Oh[1] · **Jae Moon Kim**[1] · **Chin Young Chang**[1]

Received: 6 November 2023 / Revised: 6 February 2024 / Accepted: 22 February 2024 / Published online: 18 March 2024

Abstract
This paper presents the composition of a lithium polymer battery and a battery management system used in the configuration of 10-car urban railway vehicles on Seoul Line 4 in the Republic of Korea. The operating environment and load usage conditions are analyzed. The initial capacity was measured through full charge/full discharge experiments, and the battery capacity after the experiment was measured and used as training data. During railway vehicle operation, the battery load characteristic is that power is supplied through the charger, except in certain sections. Battery usage is extremely short compared to the operating time, and floating charging is constantly performed through the charger. Under these conditions, a battery aging experiment was conducted over 500 cycles. To minimize the impact of aging due to capacity measurements, the battery's capacity was measured every 100 cycles. The experiments were performed at room temperature to replicate conditions similar to those of actual vehicles. The acquired data were preprocessed to enhance the accuracy of state of health (SoH) estimation. The SoH of the battery was then estimated using a long short-term memory model, which is a type of deep learning recurrent neural network.

Keywords Lithium polymer battery · State of health (SoH) · Long short-term memory (LSTM) · Urban railway vehicle

1 Introduction

In a railway vehicle, the battery serves as a fundamental power source that sustains the vehicle. It is utilized for initial operation, control power, and emergency power. Lead-acid, nickel-cadmium, and lithium batteries are widely used in railway vehicles, and lithium polymer batteries have recently been applied owing to their efficiency and safety [1]. Railway vehicle batteries are used in situations in which power cannot be supplied using overhead lines or during initial startup. Therefore, unless under special circumstances that involve prolonged power supply interruptions owing to faults, batteries have low power consumption and exhibit a low depth of discharge (DoD). Lithium polymer batteries have a short history of usage in railway vehicles; therefore, there exists a lack of research on their replacement timing and remaining life prediction considering the load characteristics of the vehicle. In addition, for lithium batteries, research has primarily been conducted on the cell-level state of charge (SoC) and state of health (SoH) estimation [2–6], and little research has been conducted on the actual applied module or pack level.

Chao Lyu's [7] research utilizes a time domain Electrochemical Impedance Spectroscopy (EIS) measurement technique and equivalent circuit model interpretation to estimate the State of Health of Lithium-ion Batteries (LIBs). This study introduces a Fast-EIS measurement method, which includes a frequency-mixing measurement algorithm based on Fast Fourier Transform (FFT). This method enhances the speed of EIS measurements and improves the accuracy of SOH estimation.

for LIBs. However, it is difficult to apply the proposed method because the battery of the railway vehicle is not easily detachable, and the application is challenging due to the varying usage environment depending on the season and

✉ Jae Moon Kim
goldmoon@ut.ac.kr

✉ Chin Young Chang
ccy9247@ut.ac.kr

Hyo Seok Oh
gy0444@ut.ac.kr

[1] Transportation System Engineering, Korea National University of Transportation, 157 Cheoldobangmulgwan-ro, Uiwang-si, Gyeonggi-do 16106, Republic of Korea

time. Ji'ang Zhang's research in [8] presents the LSSVM-ECM method for estimating the State of Health (SOH) of lithium-ion batteries. The LSSVM-ECM combines an empirical degradation model (EDM) with a data-driven approach to address both overall and local battery degradation trends. Validation with Oxford and NASA datasets confirms its high accuracy and robustness. YongZhi Zhang's research in [9] applies deep learning, specifically the Long Short-Term Memory (LSTM) recurrent neural network, to predict the Remaining Useful Life (RUL) of lithium-ion batteries. The LSTM RNN model is adaptively optimized using the resilient mean square back-propagation method, successfully capturing long-term dependencies among degraded battery capacities, resulting in more accurate RUL predictions. Nevertheless, the aforementioned studies were conducted at the battery cell level and did not account for real-world environmental factors, such as temperature variations and actual load usage profiles that batteries encounter in practical applications.

In this study, a lithium-polymer battery pack (Pack) used in urban railway vehicles was configured along with a battery management system (BMS) and charging method.

Additionally, the experimental conditions were applied after analyzing the battery usage time and types of loads powered by the battery, which are influenced by the operational characteristics of railway vehicles.

Furthermore, considering that the actual battery is located underneath the vehicle, where it is exposed to external temperatures, the experiments were conducted at room temperature. Temperature data were measured during the experiments.

The state estimation factors were derived using the experimentally measured battery voltage, current, and temperature data. The long short-term memory (LSTM) model, a type of deep learning model, was employed to estimate the SoH.

2 Battery System for Railway Vehicles

2.1 Battery Charger

Battery charging methods can be categorized into five types: trickle charging, equalizing charging, float charging, normal charging, and fast charging. Other purposes include recovery of charging and initial charging.

Trickle Charging is a method where a minimal current is applied to the battery in the off state to replenish self-discharge and maintain a continuous charge. Equalizing Charging is a method used to compensate for cell-level potential differences caused by variations in internal resistance. In the floating charging method, the charger and battery are constantly connected, with the charger supplying power for the commercial load and battery charging, while the battery supplies high power that would be difficult for the charger to supply. Fast Charging is a method that involves charging at 2 to 3 times the normal charging current within a short period, impacting battery life and characteristics. Recovery Charge is a method designed to restore the electrode plates of a battery that has been left in a discharged state for an extended period. Initial Charge is a charging method used to achieve optimal performance when using the battery for the first time. The battery charging method for railway vehicles is typically implemented using a floating charging method [10].

In this study, a battery charging device for a railway vehicle was supplied with three-phase alternating current power through a static inverter (SIV) and controlled by an DC/AC-AC/DC converter using insulated-gate bipolar transistor (IGBT) devices. Through control, the battery charging device outputs a DC voltage of 100 V, which charges the battery at a constant voltage (CV) (Fig. 1). The battery charging units were connected in parallel to supply power for the battery charging and DC loads. It comprises three chargers and three battery packs, following a standard of a 10-car train configuration.

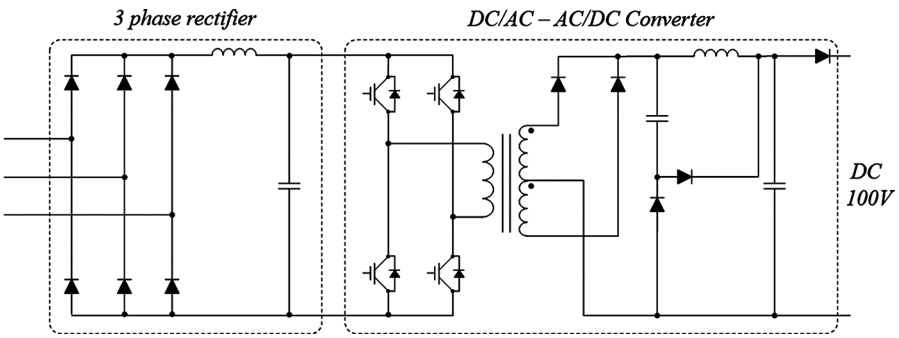

Fig. 1 Battery Charger configuration

Table 1 Railway vehicles battery specifications

Item	Specification	
Battery Type	Lithium Polymer	
Configuration	Cell Parallel, Module Series	Module 1: Cell 2 P 9 S Module 2: Cell 2 P9 S Module 3: Cell 2 P 7 S
Nominal Voltage	DC 91.25 V	DC 3.65 V X 25Cells
Rated Capacity	106Ah	53Ah * 2P
Operating Voltage	DC 75~103.75 V	
Charging Method	Constant Voltage(CV)	
Maximum Charging Current	115 A	Protection Standard
Maximum Charging Voltage	DC 103.75 V	DC 4.15 V X 25Cells
Charging Terminal Voltage	DC 103.75 V	
Discharge Method	Constant Current(CC)	
Maximum Discharge	230 A	Protection Standard

2.2 Battery Module

The battery used in the experiment was composed of a battery pack and a battery management system (BMS) applied to the Seoul subway Line 4 (Republic of Korea); the specifications of the battery pack are listed in Table 1.

Figure 2 illustrates the protective circuit within the battery pack used for charging and discharging. Diodes are used to prevent a reverse current flow during charging or discharging. The contactor (CK) physically disconnects the connection between the external load and the charger during overcharging, over-discharging, or high temperatures to protect the battery. The high-power resistor limits the current to prevent damage caused by overcharging and inrush currents during discharge. During discharging, Pre_DCK prevents the initial inrush current; subsequently, the current is sent directly to the load through DCK.

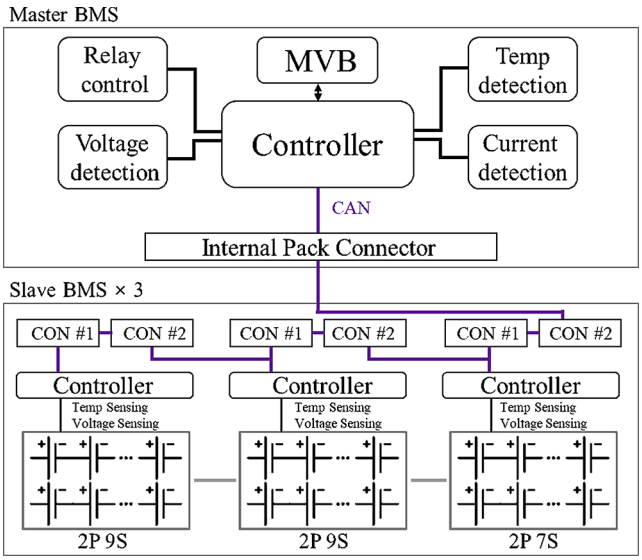

Fig. 3 BMS Block Diagram and Internal Structure

2.3 Battery Management System, BMS

The BMS was equipped with one Slave BMS for each of the master BMS and three battery modules. The master and slave BMS are connected for slave BMS operation with +12 V power and CAN communication. The slave BMS transmitted the voltage and module temperature of each battery cell to the Master BMS via CAN communication. The Master BMS acquires the battery voltage, current, and temperature information and controls the contactor to protect the battery. Figure 3 illustrates the block diagram and internal system structure of the master and slave BMS. The battery module comprises three modules, each of which obtains the cell voltage through the slave BMS and performs cell balancing based on the acquired data.

The master BMS measured the temperature, input voltage, and input/output currents of the battery module. The voltage of the battery pack was calculated using the data obtained from the slave BMS. Moreover, it executes battery protection operations based on the conditions of the BMS, as listed in Table 2. Furthermore, the BMS implemented in railway vehicles stores data such as voltage, current, temperature, and SoC. However, estimating battery aging based

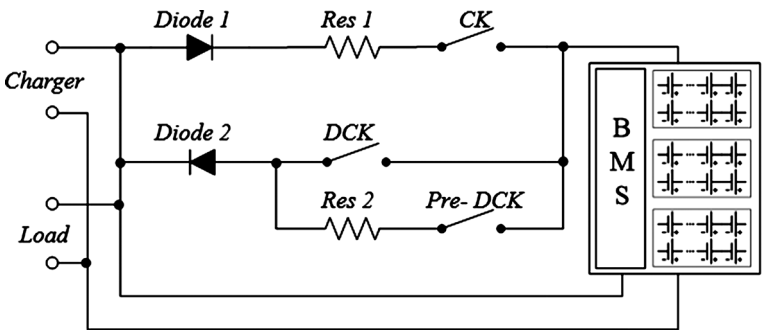

Fig. 2 Battery charge/discharge circuit

Table 2 BMS protection operation

Item		Protection circuit cutoff	Return condition
Over-charging cell voltage cutoff		Over 4.25 V for 5s	Below 4.0 V
Over-charging pack voltage cutoff		Over 106.25 V for 5s	Below 100 V
Over-discharge cell voltage cutoff		Below 2.9 V for 5s	Over 3.2 V
Over-discharge pack voltage cutoff		Below 72.5 V for 5s	Over 80 V
Charge overcurrent cutoff	Over 3.5 V	Over 115 A for 5s	Over 5 A discharge
	Below 3.5 V	Over 150 A for 5s	
Discharge overcurrent cutoff		Over 230 A for 5s Over 350 A	Below 100 A Over 5 A charge

on the results of an open-circuit voltage (OCV) experiment conducted on an early designed cell is difficult. Therefore, this paper proposes a technique for estimating the SoH using data that can be acquired with a BMS.

3 Analysis of Railway Vehicle Operation Environment

3.1 Load Characteristic Analysis

The batteries of urban railway vehicles are primarily used for DC loads ranging from 75 to 100 V, serving as power sources for the initial operating and control units. Most loads used for batteries in urban railway vehicles encompass DC loads, which are organized in parallel and connected to a battery charger. Battery charging was performed consistently using a floating charging method. During urban railway vehicle operation, the power from the charger is used as the power source for DC loads. In this study, we examined the types and capacities of battery loads under normal operating conditions using a 10-car train for urban railway vehicles for battery aging experiments. The types of direct current loads for Seoul Line 4 urban railway vehicles are listed in Table 3. There were approximately 67 types of electric device controllers, broadcasting indicators, registers, and other DC loads [10, 11, 12, 13]..

Under normal vehicle conditions, the battery load was applied at a load rate of 13,413 W, as listed in Table 1. Loads were distributed among the three battery packs; therefore, each battery pack supplies 4,471 W of load power. Therefore, if the rated voltage of one battery pack is calculated as 91.25 V, the current capacity output from one battery pack is approximately 50 A.

3.2 Battery Usage Time Analysis for One Day

In urban railway vehicles, the battery serves as the power source for all DC loads within the vehicle during the initial maneuvers when there is no power supply through the pantograph. The controller's "ON" signal activates the DC load, and the auxiliary air compressor starts, creating pressure in the auxiliary air supply and pantograph air supply through the auxiliary air duct. The air pressure from the auxiliary reservoir raises the pantograph, which is the current collector, and makes contact with the overhead lines to receive power.

The air reservoir and conduits of the auxiliary air system were pressurized by pneumatic filling. The auxiliary air compressor motor operated at 100 V DC power until the air pressure required to raise the pantograph was reached. When powered by the battery, the air pressure of the auxiliary air system reaches 7.5 kg/cm², at which point the auxiliary air compressor motor is stopped. The use of battery power to fill the auxiliary air compressor requires approximately 8 min and occurs once per day on average. Furthermore, during urban railway vehicle operation in insulated

Table 3 Battery load capacity of railway vehicles

NO.	Device Name		Quantity (1 unit)	unit Power Consumption [W]	Operating Rate	Load Power [W]
1	SIV	Controller	3	900	0.70	630
2	Lights	Initial	236	6,372	0.05	319
3		continuity	80	2,160	0.95	2,052
⋮	⋮		⋮	⋮	⋮	⋮
33	Auxiliary Compression Motor		3	1,200	0.25	300
⋮	⋮		⋮	⋮	⋮	⋮
63	CBM	Data server	2	300	0.70	210
64	(Condition Based Maintenance)	CBM IO module	10	1,000	0.70	700
65		Truck IO module	20	300	0.70	210
66		Relay	2	156	1.00	156
67		Indicator Lamp	2	100	1.00	100
Battery load capacity						13,413

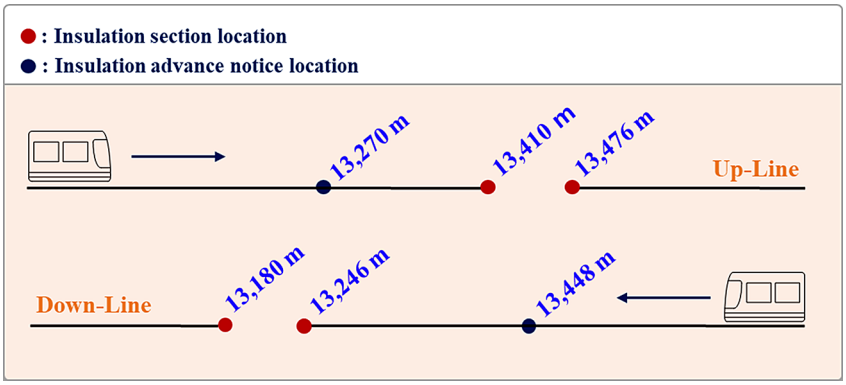

Fig. 4 Railway vehicle insulation section operation chart

Table 4 Average railway vehicle battery usage time/day

Item	Average time/day
Auxiliary Compression Motor operation	8 min
Insulation section	2.9 min (174.24 s)
Average speed of passage	40 km/h

sections, where power from overhead lines is not supplied, the DC load receives power solely from the battery [10].

The urban railway vehicle investigated in this study is operated in a power system that combines AC and DC sections. The track section was supplied with single-phase AC at 25 kV 60 Hz and a direct current of 1,500 V. Hence, there were insulated sections between the track connection segments with different power systems. Figure 4 illustrates the railway vehicle insulation section operation chart for the target vehicle, and Table 4 presents the corresponding battery usage times for various railway vehicle operating environments.

$$\left(\frac{13{,}485-13{,}270}{40?km/h}+\frac{13{,}448-13{,}179}{40?km/h}\right)\times 4=174.24\,[sec]\,(1)$$

Equation (1) represents the calculated duration of the insulated section passage based on the assumption of four daily operations. To determine the discharge time for the lithium battery aging experiment, considering the operational conditions of railway vehicles, we selected 12 min by combining the ACM activation time and insulated section time with a 10% margin applied for 10.9 min.

Table 5 Bidirectional power supply specifications

Item	Specification
Voltage range	0 ~ 200 V
Current range	0 ~ 140 A
Max power	10 kw
Load type	Electronic-Load

4 Battery Experiment

4.1 Battery Capacity Measurement

Figure 5 illustrates the experimental setup utilized for battery charging and discharge experiments. The setup comprises a computer responsible for experiment control and data collection from each battery cell. Additionally, it includes a bidirectional power supply unit tasked with managing the charging and discharging processes of the battery. Table 5 provides the specifications of the bidirectional power supply unit. The charging and discharging of the battery involved connecting the anode of the battery pack to a bidirectional

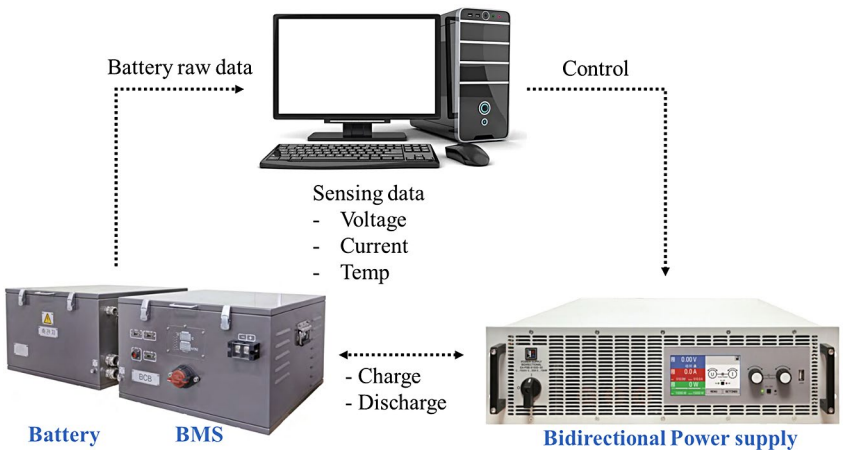

Fig. 5 Battery experiment diagram

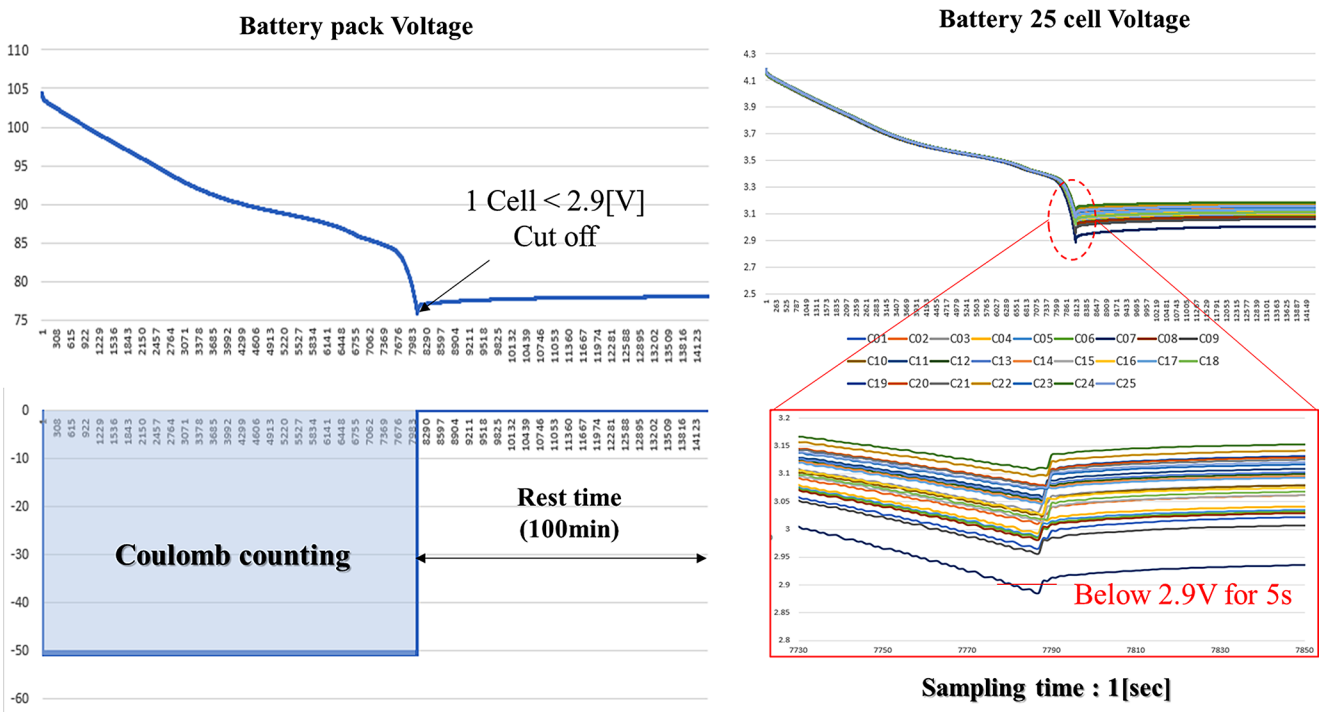

Fig. 6 Capacity Measurement experimental waveform

power supply unit, and controlling the bidirectional power supply unit through a computer. Key information such as voltage, current, and temperature data for each battery cell was collected at 1-second intervals through a communication interface with the BMS.

Furthermore, the initial capacity of the battery was determined by confirming the actual initial capacity through charge and discharge experiments, not by using the nominal capacity from the design. The initial capacity estimation method applies the current integration method represented in Eq. (2).

$$C = \frac{1}{3600}\int_0^t i_{batt}(t)\,dt\,[Ah] \quad (2)$$

where C = Battery capacity, i_{batt} = battery discharge current.

The full charge and full discharge conditions of the battery were set to the cell protection criteria implemented by the BMS, with the upper and lower voltage limits set at 4.25 V and 2.9 V, respectively. Additionally, the experiments were conducted with a load current of CC-DC 50 A for a single battery pack, and adequate rest time was provided to ensure battery stability.

Figure 6 shows the full discharge of the battery. When the cell voltage dropped below DC 2.9 V, the load was disconnected 5 s later to prevent current flow. Furthermore, while the cell voltages initially exhibited similar patterns, as the complete discharge approached, variations in the voltages of each cell became evident. This is because the cell balancing applied to the railway vehicle BMS is passive, resulting in a rapid increase in the voltage imbalance compared to the cell balancing speed. Table 6 presents the results of the initial capacity test for the experimental battery with an average capacity of 110.59 Ah.

Table 6 Battery initial capacity measurement results

Test	Discharge capacity [Ah] / average temp [°C]
1	110.23 / 28.7
2	110.71 / 32.8
3	110.62 / 27.2
4	110.54 / 33.4
5	110.97 / 36.4
6	110.24 / 27.7
7	110.82 / 33.4
Initial capacity	110.59 / 31.37

4.2 Battery Aging Experiment and data Analysis

The experiment was conducted based on a 10-car train configuration of railway vehicles, considering battery load, average daily battery usage time, and charging conditions. Therefore, an experiment was conducted by applying the analyzed railway vehicle operating environment, as presented in Table 7.

The State of Health (SoH) is typically calculated using the initial and current capacities obtained through full charge/discharge experiments, as shown in Eq. (3). For the

Table 7 Battery Aging Experimental Procedure

Step	Mode	Condition	Cut-off Condition
0	Rest	-	60 min
1	CC discharge	50 A	12 min
2	CV Charge	100 V	Cut-off current < 2 A
3	Rest	-	120 min

estimation of SoH, the capacity of the battery was measured at every 100-cycle interval during the battery aging experiment. This minimized the impact of battery aging caused by the full charge/discharge required for capacity measurement.

$$SoH\,[\%] = \frac{Capacity_{current}}{Capacity_{initial}} \times 100 \tag{3}$$

Figure 7 depicts the voltage and current waveforms for the battery aging experiment. The experiment was divided into three distinct segments: discharging, charging, and resting. At the initial stage of discharge, a rapid voltage drop occurs, caused by the internal serial resistance, as described in Eq. (4). Subsequently, owing to the polarization effect, it discharges nonlinearly and then discharges based on the load. The slope of the discharge was derived using Eq. (5). Furthermore, an incremental capacity analysis (ICA), an SoH estimation method, was applied to derive Eq. (6) from the voltage and current data while the battery was being charged. Additionally, temperature data were collected during the battery experiments conducted at room temperature.

$$R\,[\Omega] = \frac{\Delta V}{I} \tag{4}$$

$$Dischargeslope = \frac{\Delta dischargecurrent}{\Delta t} \tag{5}$$

$$IC\,[Ah/V] = \frac{\Delta Q}{\Delta V} = \frac{I}{\Delta V/\Delta t} \tag{6}$$

Figure 8 shows the battery condition estimation factor data. The battery aging experiment consisted of 500 cycles. Although changes in the values can be observed as the experiment progresses, in certain cases, the values do not consistently decrease or increase in a particular direction as the experiment advances. This is the result of conducting experiments at room temperature, similar to batteries installed in actual vehicles, and it reflects the influence of external temperature changes. Temperature variations has a prominent effect than changes in battery capacity in potentially reducing the accuracy of the estimation model. Accordingly, the correlation between the temperature and condition estimation factors was analyzed. Pearson correlation coefficient analysis was performed to confirm the linear relationship between the data, as shown in Eq. (7). The Pearson correlation coefficient was between 1 and −1. The closer it is to 0, the less correlation there is, and it has a positive or negative linear relationship depending on whether the coefficient is close to 1 or −1.

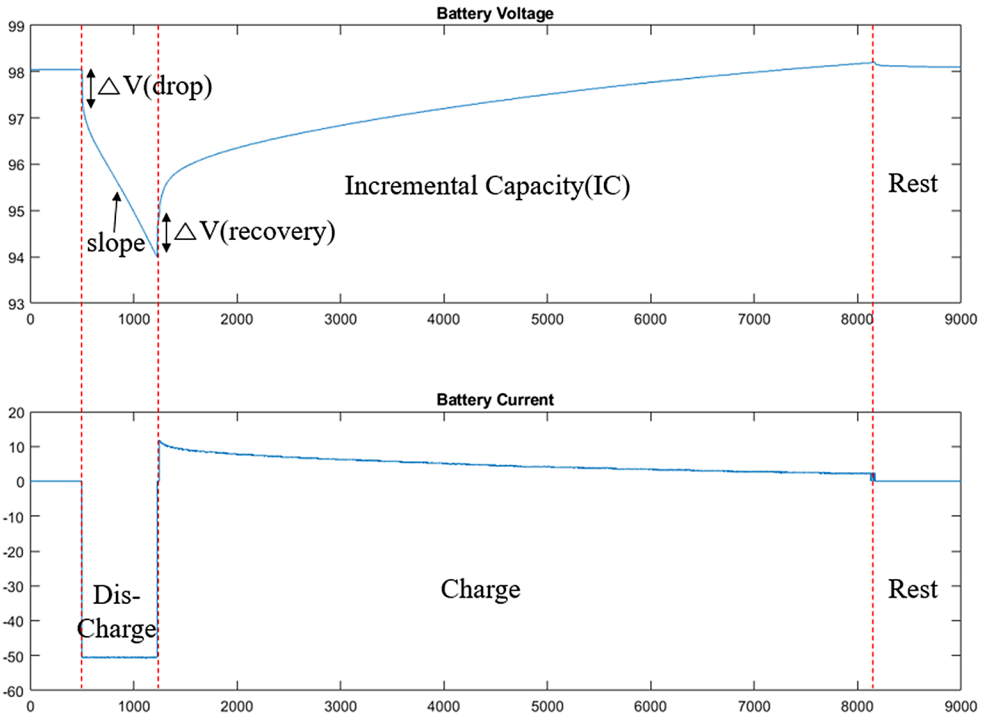

Fig. 7 Battery aging experiment wave

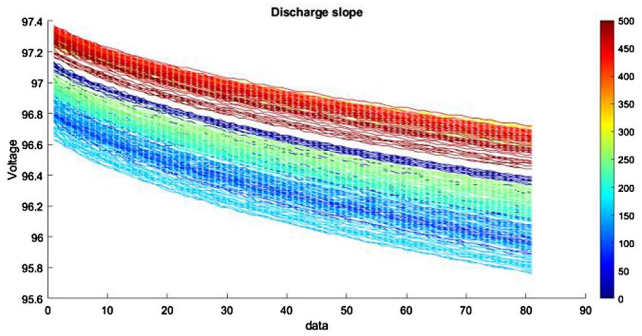

(a) Discharge slope

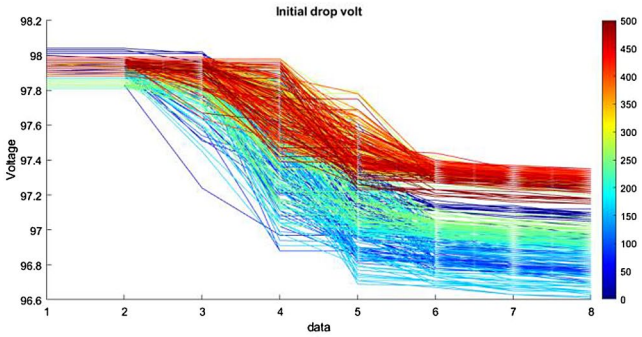

(b) △voltage

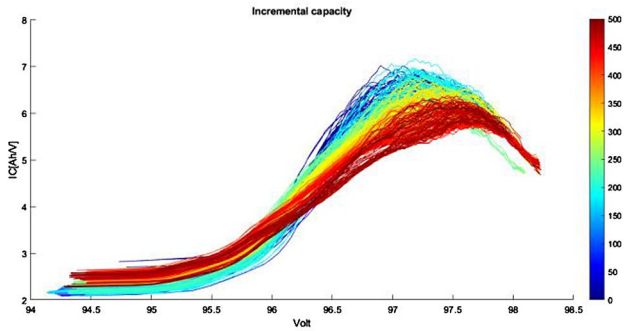

(c) Incremental Capacity

Fig. 8 Battery condition estimation factor

$$r = \frac{\sum (X - \bar{X})(Y - \bar{Y})}{\sqrt{\sum (X - \bar{X})^2 \sum \left(Y - \bar{Y}\right)^2}} \quad (7)$$

where r = correlation coefficient, X, Y = values of the two variables, $\bar{X}, \bar{Y}$ = average values of the two variables.

Fig. 9 presents the results of the correlation coefficient analysis for the condition estimation factor based on the temperature. The discharge slope and resistance exhibited a strong correlation coefficient of 0.9 or higher. Additionally, the resistance demonstrated a negative linear relationship with temperature, which is consistent with the characteristic of decreasing resistance components with increasing temperature. Factors that are sensitive to temperature changes can hinder the accurate estimation of the SoH because it is difficult to track changes due to aging.

Figure 10 shows a graph that illustrates the relationship between the discharge slope and resistance with respect to temperature. Accordingly, a temperature correction model was designed by analyzing the relationship between the temperature and the estimation factor. Additionally, a correlation coefficient analysis was conducted for the estimation factor, considering battery capacity and temperature correction. Figure 11 presents the results of the correlation coefficient analysis between the battery capacity and the estimation factors. It indicates that battery capacity is positively correlated with the incremental capacity (IC) and discharge slope, whereas it has a negative correlation with resistance. Furthermore, we selected the resistance and incremental capacity (IC), which are highly correlated with the battery capacity, and applied them to the SoH estimation model.

4.3 SoH Prediction with LSTM

In this study, the LSTM model was selected as the deep learning technique for estimating the SoH of batteries in railway vehicles. Long Short Term Memory (LSTM), a recurrent neural network model, exhibits excellent performance in processing sequential data, such as time-series data. The structure of an LSTM typically consists of three gates: an input gate that processes new information, a forget gate that decides which information to discard from the existing information, and an output gate that decides whether to output an output value. Additionally, as shown in Fig. 12, LSTM is a memory model in which four layers remember necessary information through interaction and is a deep learning technique that compensates for the problem of learning not taking place at some point when the procedure becomes long [14, 15].

Figure 13 shows a diagram of the proposed LSTM model for battery SoH estimation, which comprises three main parts: data preprocessing, training, and testing. In data preprocessing, condition estimation factors are derived from the battery data collected by the BMS, and a temperature correction model was applied. Furthermore, the data were normalized, and time-series cross-validation was conducted, which is an effective technique for evaluating the model's generalization performance while maintaining the order of the time-series data. The data are divided into consecutive 'windows,' with each window serving as a test set, and the remaining windows used as a training set to train and evaluate the model. The process helps prevent overfitting and assess the performance of the model. During the testing phase, the designed LSTM model is used to estimate the SoH of the battery. Table 8 presents the hyperparameters

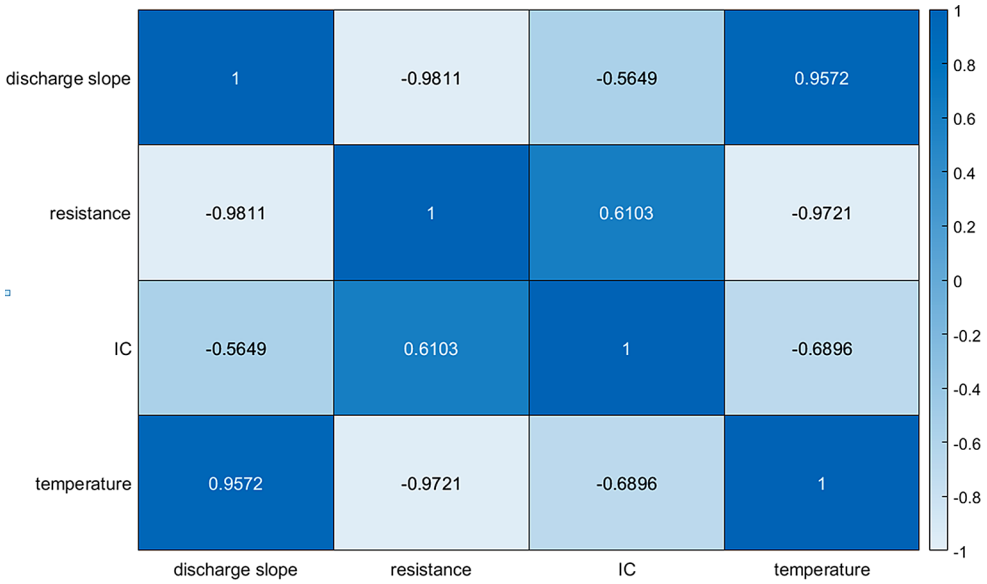

Fig. 9 Temperature-condition estimation factor correlation results

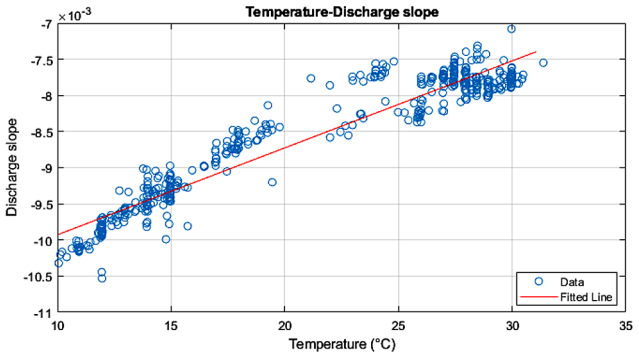

(a) Discharge slope

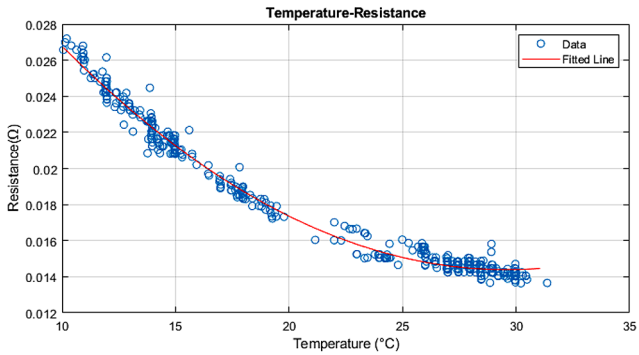

(b) Resistance

Fig. 10 Temperature- condition estimation factor graph

of the LSTM model for SoH estimation. To optimize the estimation model, training was conducted with varying values of Epochs and window size.

Fig. 14 depicts the results of the battery SoH estimation model based on LSTM. The model was trained using experimental aging data and battery capacity measurements taken every 100 cycles as references. (a) shows the original data and the model estimation results, which are zoomed in (b). (c) represents the Root Mean Square (RMSE), which is the error between the original data and the estimated data. Figure 14 shows the training results of the LSTM model with a window size set to 25%. Training was conducted with varying values of Epochs. As the number of Epochs increased, the performance of the model tended to improve. In addition, unlike the relatively linear original data, the estimated data are nonlinear, which is the result of learning from the battery capacity measured every 100 cycles, rather than learning the data by measuring the battery capacity for each experiment.

Figure 15 shows the training results of the LSTM model, which was configured with a window size of 10% to increase the range and frequency of learning. Training was conducted with varying values of Epochs. Similar to the model with a window size of 25%, as the number of Epochs increased, the performance of the model tended to improve. The RMSE results of each model's training are presented in Table 9.

As a result, it was observed that the SoH estimation performance increased when the Window Size decreased, expanding the learning range, or when the number of Epochs increased, increasing the number of learning iterations. Furthermore, the validity of the SoH estimation model for the battery was verified through the designed LSTM model.

Generally, the maintenance of railway vehicle batteries involves complete replacement when a problem occurs or when the usage period has elapsed. However, since the battery of a railway vehicle is used only under specific conditions and in emergencies, it is difficult to determine the aging of the battery. Therefore, state diagnosis techniques using battery data are essential for a systematic and efficient maintenance system. Lithium batteries are recommended

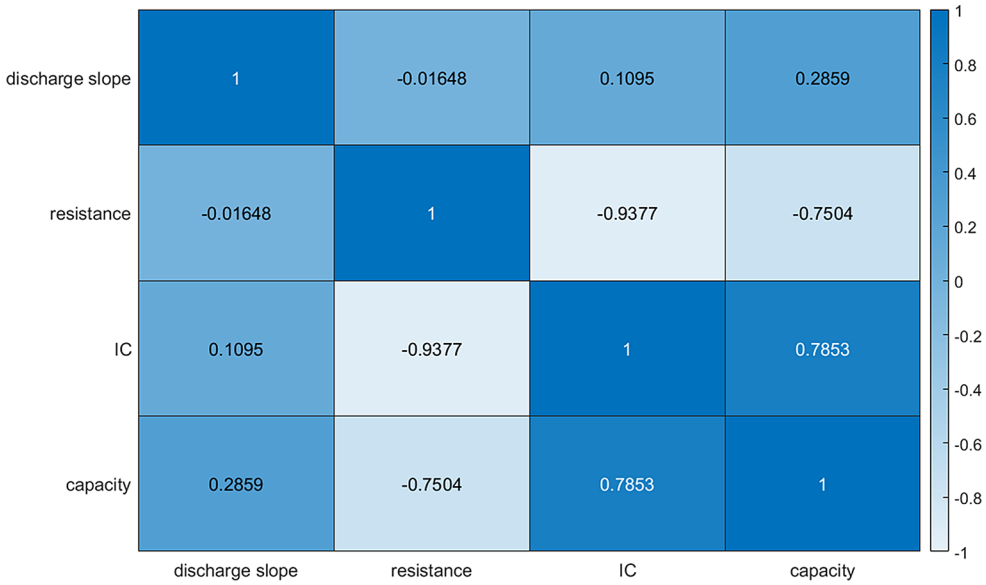

Fig. 11 Capacity-condition estimation factor correlation results

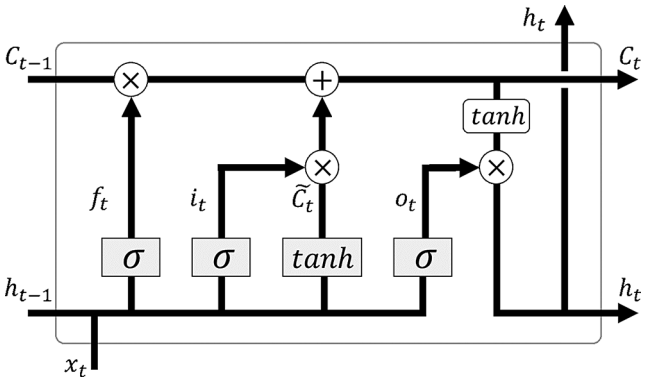

Fig. 12 LSTM Model Configuration

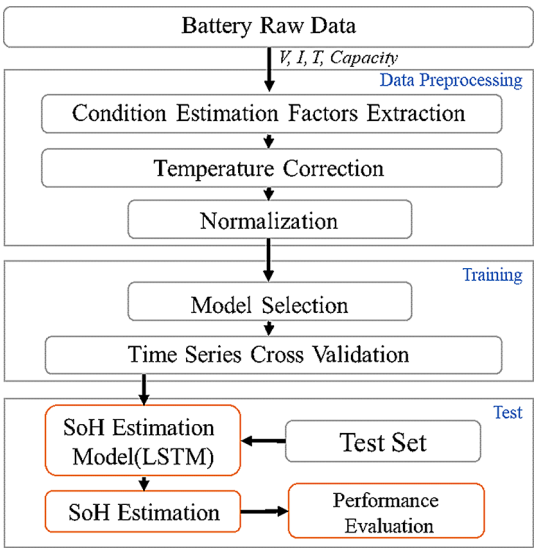

Fig. 13 SoH estimation algorithm diagram

Table 8 Hyperparameters for SoH estimation model(LSTM)

Hyperparameter	Value
Learning rate	0.005
Hidden layer	50
Dropout	0.5
Epochs	50, 100, 150, 200
Rolling window size	10%, 25%

for replacement when the capacity decreases by 20% compared to the initial capacity, as swelling can occur, and this can lead to a decrease in capacity.

5 Conclusion

In this study, the operating environment and battery loads were analyzed for domestic 10-car train urban railway vehicles using lithium batteries. During the operation of urban railway vehicles, batteries for railway vehicles supply power to loads using charging devices, except in specific sections. The battery discharge time is based on the initial operation and insulated sections. The battery supplies approximately 50 A of current to the load during discharge, and it was determined that the battery was used for an average of approximately 12 min/day, including a margin for railway vehicle operation.

A lithium battery module and BMS, which are used in urban railway vehicles, were assembled and tested using a bidirectional charging device. The BMS software was designed to enable real-time acquisition of battery voltage, current, and temperature data at 1-second intervals. Moreover, the initial capacity and the capacity measured every 100 cycles were determined via full charge and discharge experiments. Subsequently, battery aging experiments were

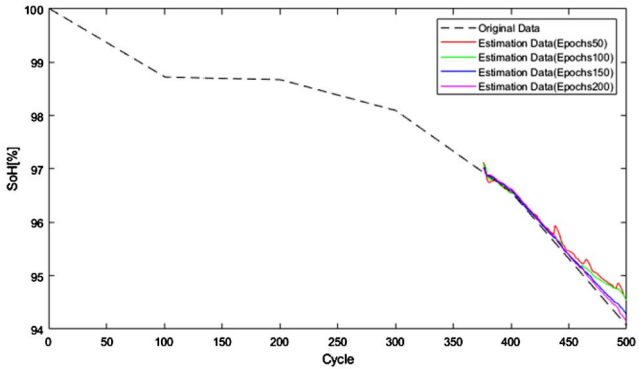

(a) Battery SoH original, estimation

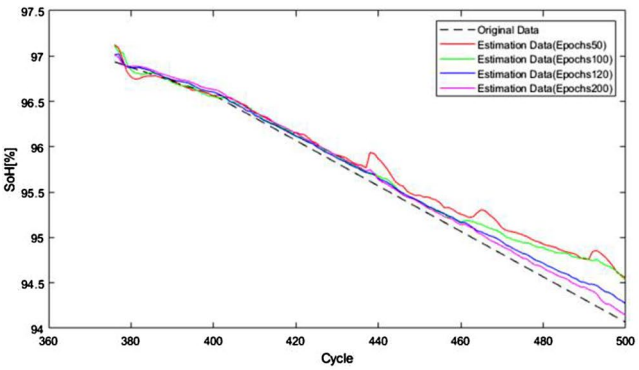

(b) Zoom (a)

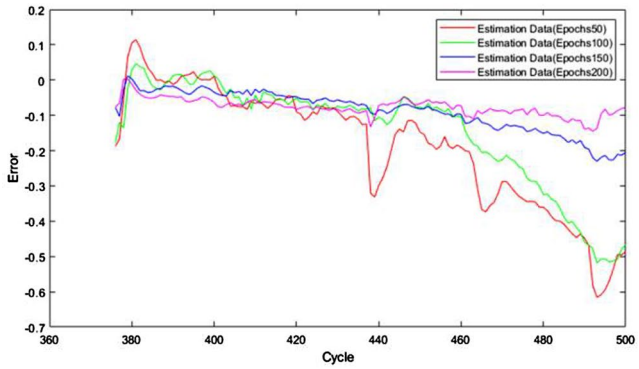

(c) Error

Fig. 14 State of Health (SoH) Estimation Results with LSTM. (Window Size 25%)

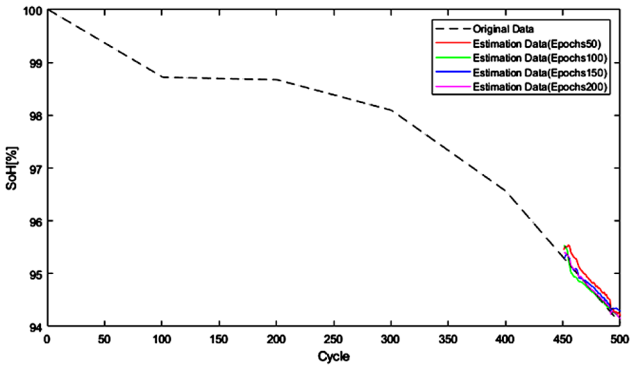

(a) Battery SoH original, estimation

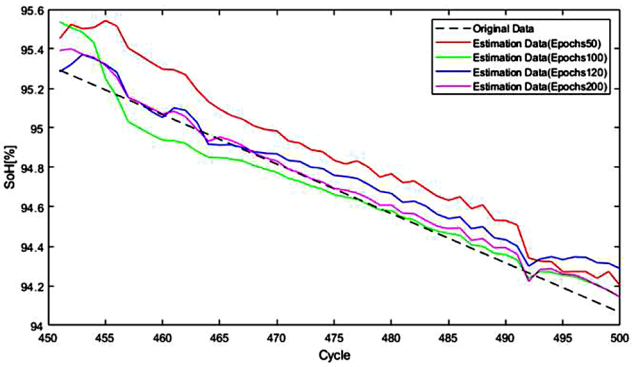

(b) Zoom (a)

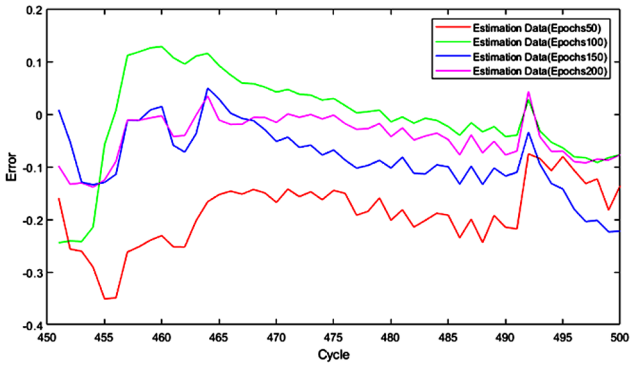

(c) Error

Fig. 15 State of Health (SoH) Estimation Results with LSTM. (Window Size 10%)

Table 9 Estimation results(RMSE) of LSTM

Epochs	Window Size	
	25%	10%
50	0.2543	0.1971
100	0.2096	0.1046
150	0.1055	0.0910
200	0.0801	0.0607

conducted considering the railway vehicle operating conditions. The condition estimation factors that could be used to estimate the condition of the battery were derived from the aging experiment data. Temperature correction was applied based on correlation analysis with temperature. Subsequently, the condition factors for the SoH estimation model were derived, and the SoH of the battery was estimated using the LSTM model, which is a deep learning technique. The results showed that the most superior model had an RSME of 0.0607, validating the effectiveness of the SoH estimation battery state diagnosis designed based on data.

Furthermore, systematic maintenance is essential for railway vehicles, as significant damage can occur in the event of an accident, and the timing of battery replacement is very important. The lifespan of a railway vehicle's battery varies depending on the season and load conditions. Therefore, while the battery recommendations from the manufacturer should be considered, it is necessary to determine the timing and tightness of battery replacement considering the characteristics of the railway vehicle and the time available in case of an emergency.

Acknowledgements This work was supported by the Korea Agency for Infrastructure Technology Advancement (KAIA) by the Ministry of Land, Infrastructure and Transport under Grant 22RSCD-A165903-03.

References

1. Cho K-H, Kang S-W (2016) A Study on the Rail Vehicle Applications and Increase the Capacity of Lithium Polymer Batteries, The Transactions of the Korean Institute of Electrical Engineers Vol. 65, No. 4, pp. 340–345
2. Brady M (2017) Assessment of Battery Technology for Rail Propusion Application, U.S Department of Transportation FRA(Federal Railroad Administration), pp. 4–68
3. Wei J, Chen C (2020) State of Charge and Health Estimation For Lithium-Ion Batteries Using Recursive Least Squares. In 2020 5th International Conference on Advanced Robotics and Mechatronics (ICARM), 686–89. Shenzhen, China: IEEE, https://doi.org/10.1109/ICARM49381.2020.9195346
4. Shen P, Ouyang M, Lu L, Li J (2016) State of Charge, State of Health and State of Function Co-Estimation of Lithium-Ion Batteries for Electric Vehicles. In 2016 IEEE Vehicle Power and Propulsion Conference (VPPC), 1–5. Hangzhou, China: IEEE, https://doi.org/10.1109/VPPC.2016.7791782
5. El Mejdoubi A, Oukaour A, Chaoui H, Gualous H, Sabor J, Slamani Y (April 2016) State-of-charge and state-of-health Lithium-ion batteries' diagnosis according to Surface temperature variation. IEEE Trans Industr Electron 63(4):2391–2402. https://doi.org/10.1109/TIE.2015.2509916
6. Azis N, Ayzah E, Joelianto, Widyotriatmo A (2019) State of Charge (SoC) and State of Health (SoH) Estimation of Lithium-Ion Battery Using Dual Extended Kalman Filter Based on Polynomial Battery Model. In 2019 6th International Conference on Instrumentation, Control, and Automation (ICA), 88–93. Bandung, Indonesia: IEEE, https://doi.org/10.1109/ICA.2019.8916734
7. Lyu C, Zhang T, Luo W, Wei G, Ma B, Wang L (2019) SOH Estimation of Lithium-Ion Batteries Based on Fast Time Domain Impedance Spectroscopy. In 2019 14th IEEE Conference on Industrial Electronics and Applications (ICIEA), 2142–47. Xi'an, China: IEEE, https://doi.org/10.1109/ICIEA.2019.8834119
8. Zhang J, Wang P, Gong Q et al (2021) SOH estimation of lithium-ion batteries based on least squares support vector machine error compensation model. J Power Electron 21:1712–1723. https://doi.org/10.1007/s43236-021-00307-8
9. Zhang YZ, Xiong R, He HW, Liu Z (2017) A LSTM-RNN Method for the Lithuim-Ion Battery Remaining Useful Life Prediction. In 2017 Prognostics and System Health Management Conference (PHM-Harbin), 1–4. Harbin, China: IEEE, https://doi.org/10.1109/PHM.2017.8079316
10. Kim JY (2023) A Study on SoH Estimation of Lithium Battery Considering Load Characteristics of Electric Railway Vehicles, Ph.D. dissertation, Korea National University of Transportation
11. Oh HS et al (2023) A Study on the SoC of Lithium Battery Applied to the Operating Environment of Urban Railway Vehicle. The Transactions of the Korean Institute of Electrical Engineers, vol. 72, no. 5, pp. 662 ~ 668
12. He J, Wei Z, Bian X, Yan F (June 2020) State-of-health estimation of Lithium-Ion batteries using Incremental Capacity Analysis based on voltage–capacity model. IEEE Trans Transp Electrification 6(2):417–426. https://doi.org/10.1109/TTE.2020.2994543
13. Stroe D-I and Erik Schaltz. Lithium-Ion Battery State-of-health estimation using the incremental capacity analysis technique. IEEE transactions on industry applications 56, 1 (January 2020): 678–685. https://doi.org/10.1109/TIA.2019.2955396
14. Park K, Choi Y, Choi WJ, Ryu H-Y, Kim H (2020) LSTM-Based battery remaining useful life prediction with Multi-channel charging profiles. IEEE Access 8:20786–20798. https://doi.org/10.1109/ACCESS.2020.2968939
15. Zhang L, Ji T, Shihao Yu, and, Liu G (2023) Accurate Prediction Approach of SOH for Lithium-Ion batteries based on LSTM Method. Batteries 9, 3 (March 18. 177. https://doi.org/10.3390/batteries9030177

Hyo Seok Oh received the B.S. degree in Mechatronics engineering from the Induk University, Korea, in 2020, and then received M.S. degree from Korea National University of Transportation in 2022, Since 2022, he has been with Korea National University of Transportation, where he is currently a Ph.D. course. His research interest is power electronics of railway.

Jae Moon Kim received the B.S degree in 1994 and the Ph.D. degree in 2000 from Sungkyunkwan University. From 2004 to 2011, he was with the department of rolling stock electrical engineering, Korea National Railroad College. Since 2012, he has been with the department of transportation engineering in the transportation graduated school, KNUT. His research interests are power conversion in industry fields, traction and regeneration control in electric railway.

Chin Young Chang received the M.S. degree from Chung-Ang University Graduate School in 2010 and the Ph.D. degree in 2015 from Chung-Ang University Graduate School. Since March 2012, he has been working as a research assistant in the Department of Transportation System Engineering at Korea National University of Transportation. His research interest is power electronics of railway.